

RESEARCH LETTER

10.1002/2017GL073486

Key Points:

- A simulated Lambert-Amery glacial system contributed a range of +3.6 to −117.5 mm global mean sea level equivalent over 500 years
- The Lambert-Amery glacial system maintains stability while a small ice shelf remains to buttress the ice flow
- Resolving ice flow through narrow channels in the Lambert-Amery glacial system is important for investigating its future stability

Supporting Information:

- Supporting Information S1

Correspondence to:

M. L. Pittard,
mark.l.pittard@durham.ac.uk

Citation:

Pittard, M. L., B. K. Galton-Fenzi, C. S. Watson, and J. L. Roberts (2017), Future sea level change from Antarctica's Lambert-Amery glacial system, *Geophys. Res. Lett.*, *44*, 7347–7355, doi:10.1002/2017GL073486.

Received 17 MAR 2017

Accepted 13 JUN 2017

Accepted article online 16 JUN 2017

Published online 29 JUL 2017

Future sea level change from Antarctica's Lambert-Amery glacial system

M. L. Pittard^{1,2} , B. K. Galton-Fenzi^{2,3} , C. S. Watson⁴ , and J. L. Roberts^{2,3} 

¹Institute for Marine and Antarctic Studies, University of Tasmania, Hobart, Tasmania, Australia, ²Antarctic Climate & Ecosystems Cooperative Research Centre, University of Tasmania, Hobart, Tasmania, Australia, ³Australian Antarctic Division, Kingston, Tasmania, Australia, ⁴School of Land and Food, University of Tasmania, Hobart, Tasmania, Australia

Abstract Future global mean sea level (GMSL) change is dependent on the complex response of the Antarctic ice sheet to ongoing changes and feedbacks in the climate system. The Lambert-Amery glacial system has been observed to be stable over the recent period yet is potentially at risk of rapid grounding line retreat and ice discharge given that a significant volume of its ice is grounded below sea level, making its future contribution to GMSL uncertain. Using a regional ice sheet model of the Lambert-Amery system, we find that under a range of future warming and extreme scenarios, the simulated grounding line remains stable and does not trigger rapid mass loss from grounding line retreat. This allows for increased future accumulation to exceed the mass loss from ice dynamical changes. We suggest that the Lambert-Amery glacial system will remain stable or gain ice mass and mitigate a portion of potential future sea level rise over the next 500 years, with a range of +3.6 to −117.5 mm GMSL equivalent.

1. Introduction

The projected global increase in temperature over the next 500 years varies between 0°C and 10°C, depending on greenhouse gas emission scenarios from anthropogenic sources [Pachauri *et al.*, 2014]. The mean global temperature increases from the Representative Concentration Pathway (RCP) scenarios in the Intergovernmental Panel on Climate Change's 5th Assessment Report (AR5) (100 years and 500 years, respectively) are RCP2.6 (1.0°C, 0.5°C), RCP4.5 (1.8°C, 2.5°C), RCP6.0 (2.2°C, 3.5°C), and RCP8.5 (3.7°C, 7.5°C) [Pachauri *et al.*, 2014]. The expected response to the Antarctic ice sheet under these warming scenarios is uncertain, with the range of maximum GMSL-equivalent contribution estimates varying between 3 m [Golledge *et al.*, 2015] to 10 m [DeConto and Pollard, 2016] until 2300, and over 15 m SLR equivalent by 2500 [DeConto and Pollard, 2016]. Antarctic ice sheet simulations, which predict future sea level rise, have the current disadvantage of necessarily using relatively coarse horizontal resolution (10–20 km horizontal resolution), in addition to adopting Antarctic-wide parameterizations of unresolved physics that are not necessarily appropriate for all regions [Huybrechts, 2002; Martin *et al.*, 2011; Golledge *et al.*, 2015; DeConto and Pollard, 2016].

The Lambert-Amery glacial system features the third largest ice shelf, the Amery Ice Shelf, which borders the East Antarctic ice sheet (Figure 1a). The Amery Ice Shelf occupies a long and relatively thin embayment, which after the initial flotation narrows over the first ~60 km to a width of ~35 km, leading to a minimum in surface velocity on the ice shelf (minimum ice shelf width (MISW), Figure 1b). In addition to the MISW, there are a number of significant pinning points and other regions of regrounding within the Amery Ice Shelf, for example, Clemence Massif and the Budd Ice Rumples (Figure 1b). These features dictate that the Amery Ice Shelf is substantially different from the Ross and Ronne-Filchner Ice Shelves, which are situated in relatively wide embayments. The three major tributary glaciers of the Amery Ice Shelf, the Lambert, Mellor, and Fisher Glaciers, all flow between nunataks with glacier widths as narrow as 30 km, before converging into the rear of the Amery Ice Shelf.

Antarctic ice sheet models [Winkelmann *et al.*, 2012; Golledge *et al.*, 2015; DeConto and Pollard, 2016] are unlikely to sufficiently resolve either Clemence Massif (a nunatak ~25 km × ~10 km) or the MISW (~35 km wide flow path). Simulating a mid-ice shelf slowdown at this location is an important criteria for being able to accurately simulate the Lambert-Amery glacial system. These features are important to the flow of the Amery Ice Shelf and its tributary glaciers [Favier *et al.*, 2012] and are not sufficiently resolved with models with greater than 10 km resolution or with Antarctic-wide parameterizations.

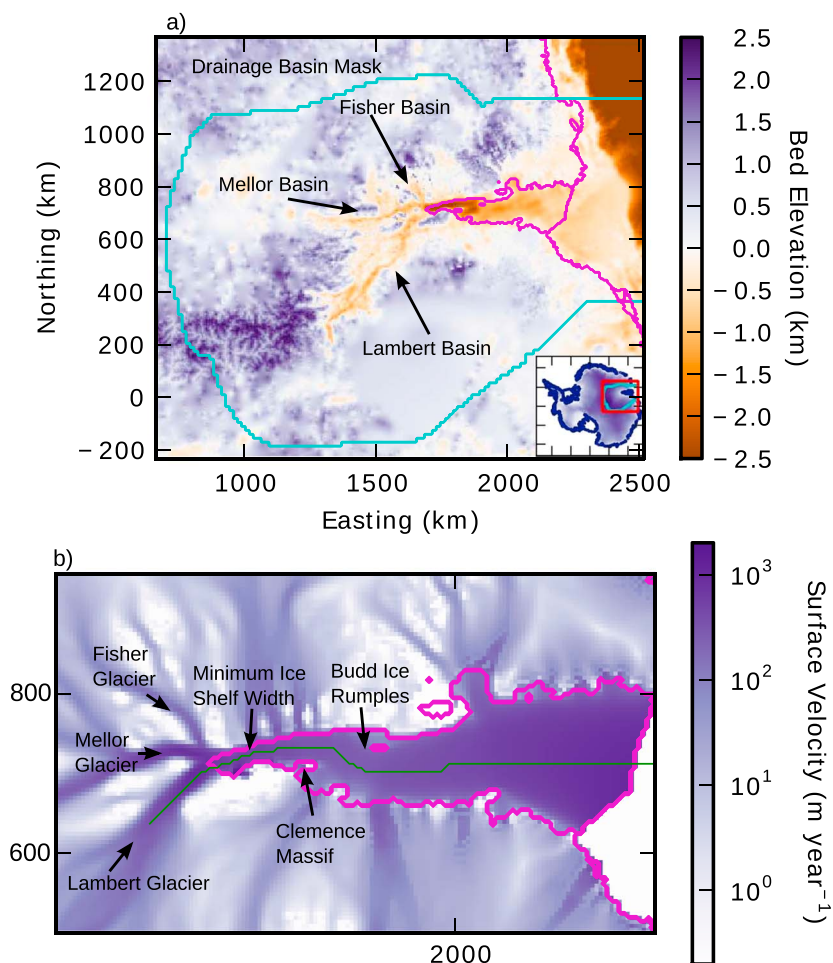


Figure 1. (a) Locality map showing the bed topography used (see supporting information S1) in the regional model of the Lambert-Amery glacial system. The full model domain is shown with red outline in the inset, the cyan line shows the drainage basin mask. (b) Control surface velocities [Pittard et al., 2016a] and main contributory glaciers and relevant features. Magenta line indicates the ocean and ice shelf boundaries, green line is the location of transect featured in Figure 2b.

The grounding line of the Amery Ice Shelf is grounded north of the MISW in Winkelmann et al. [2012] and Golledge et al. [2015]. DeConto and Pollard [2016] have a grounding line which is south of the MISW; however, the velocities in their model along the Amery Ice Shelf are lower than the observed velocities. Recent studies using either an adaptive mesh with high resolution at the grounding line [Gong et al., 2014], or a revised parameterization with finer horizontal resolution (5 km) of ice flow [Pittard et al., 2016a], yielded a realistic grounding line position in a regional simulation and resolve the flow through the MISW.

Using the Parallel Ice Sheet Model (PISM) [Bueler and Brown, 2009; Winkelmann et al., 2011; Aschwanden et al., 2012], a high-resolution regional domain of the Lambert-Amery glacial system is simulated. We simulate the effect of a series of plausible future warming and extreme scenarios, investigating the stability of the grounding line and provide an estimate for the range of GMSL change from the Amery-Lambert glacial system over the next 500 years.

2. Methods

2.1. Regional Model

The model domain and drainage basin mask is shown in Figure 1a. Outside of the drainage basin mask, the ice thickness is held constant by adjusting the surface mass balance to maintain the initial ice thickness (details in Pittard et al. [2016b]). The drainage basin mask is shifted 50 km outside of the ice divides, with the model optimization process defining the location of the ice divides within the domain. This approach allows for the

ice divides to migrate based on changes within the Lambert-Amery glacial system and ensures that no ice flows into the domain from the rest of Antarctica, but it assumes that changes that may occur outside the domain will not significantly impact this region.

The bed topography is given by a combination of Bedmap2 [Fretwell *et al.*, 2013] and RTOPO [Galton-Fenzi *et al.*, 2008; Timmermann *et al.*, 2010] (see supporting information S1). The initial ice thickness was given by Bedmap2 [Fretwell *et al.*, 2013], the geothermal heat flux by a data set generated by using the Fox Maule *et al.* [2005] methodology on the M7 magnetic data field, while the surface mass balance and surface temperatures are the average fields of 1979–2013 from RACMO2.3 ANT27/2 [van Wessem *et al.*, 2014]. The melting on the underside of the ice shelves is controlled by a pressure-melting point parameterization (outlined in Winkelmann *et al.* [2011]) and combined with a scalar which changes the distribution of the melting to resemble the simulations of the Amery Ice Shelf cavity [Galton-Fenzi *et al.*, 2012].

The horizontal resolution is 5 km and the vertical resolution 15 m in the control model and in all simulations. This horizontal resolution was chosen as it allows for a minimum of six grid cells through the major flow points of the three major glaciers, the Fisher, Mellor, and Lambert, in addition to the MISW. We apply the subgrid melt parameterization [Gladstone *et al.*, 2010; Feldmann *et al.*, 2014] shown in MISMIP3D to simulate hysteresis [Pattyn *et al.*, 2012], required to simulate the grounding line mechanics not captured by this resolution. Resolving the grounding line without a parameterization requires <500 m horizontal resolution, which is computationally prohibitive [Pattyn *et al.*, 2012]. The vertical resolution was applied based on a convergence study [Pittard *et al.*, 2016b].

The model was initialized by optimizing the model solution for four physical parameters (*ssa_e*, *sia_e*, *topg_to_phi*, and *pseudo_plastic_q*) and two calving parameters (*eigen_calving_k* and *minimum_calving_threshold*). The *ssa_e* controls the enhancement factor due to anisotropy within the shallow shelf approximation, which modifies the flow of floating and sliding ice. The *sia_e* controls the enhancement factor due to anisotropy within the shallow ice approximation, which modifies the rate of ice flow due to deformation. The *topg_to_phi* sets a depth-dependent parameterization for basal resistance, with deeper bedrock providing less resistance to flow, while the *pseudo_plastic_q* influences how the ice flow responds to basal resistance. The *eigen_calving_k* and *minimum_calving_threshold* determine the location and sensitivity of the calving front. The control solution was optimized by iteratively varying the parameters and minimizing the misfit (by comparing mean and RMS error for a range of surface elevation bands) to observations [Pittard *et al.*, 2016a] (see supporting information S1 for a full table of parameters). Our control simulation can reproduce the mid-ice shelf reduction in velocity, slowing by over 350 m yr⁻¹ in the region of the MISW. The slowdown in our control model (Figure S3) is still less than the observed slowdown (over 500 m yr⁻¹) as derived from image-based techniques [Pittard *et al.*, 2013].

2.2. Experiments

We use the range of future temperature scenarios that spans the possible future scenarios from the IPCC RCP experiments [Pachauri *et al.*, 2014] (+2°C, +4°C, +8°C), to test the sensitivity of the Lambert-Amery glacial system to future climate change. We apply the expected regional changes reflective of the global temperature variations to surface temperature (*stemp*), surface mass balance (*smb*), and melting at the underside of ice shelves (*bmelt*). For each future temperature scenario, we design a lower sea level contribution (lower), middle sea level contribution (middle), and upper contribution (upper) scenario reflective of the uncertainty in future precipitation changes over Antarctica.

The increase and bounds in the *smb* for each temperature scenario is guided by the IPCC AR5 precipitation increases and the Clausius-Clapeyron relation [O’Gorman and Muller, 2010]. The increase in *bmelt* is varied for the middle scenario by following an equation which estimates the increase in melting due to global temperature increase within the Amery Ice Shelf [Galton-Fenzi, 2009]. The increase in *stemp* is the same as global temperature change given the lack of high-latitude temperature intensification over Antarctica in the AR5 [see Pachauri *et al.*, 2014, Table 12.2]. Lastly, we extend the +4°C scenarios with two extreme cases (See Table S6 for full scenario details). The *extreme_1* scenario applies an enhancement to *bmelt* at the grounding line, aiming to simulate a greatly enhanced oceanic-forced basal melting at the grounding line beyond what is predicted by the ice shelf cavity modeling. The *extreme_2* scenario applies a *bmelt* rate of 100 m yr⁻¹ to the entire ice shelf, to simulate the response of the ice sheet to a sudden ice shelf collapse event, which could be caused by the hydro fracture mechanism [DeConto and Pollard, 2016]. This scenario is seen as unrealistic but

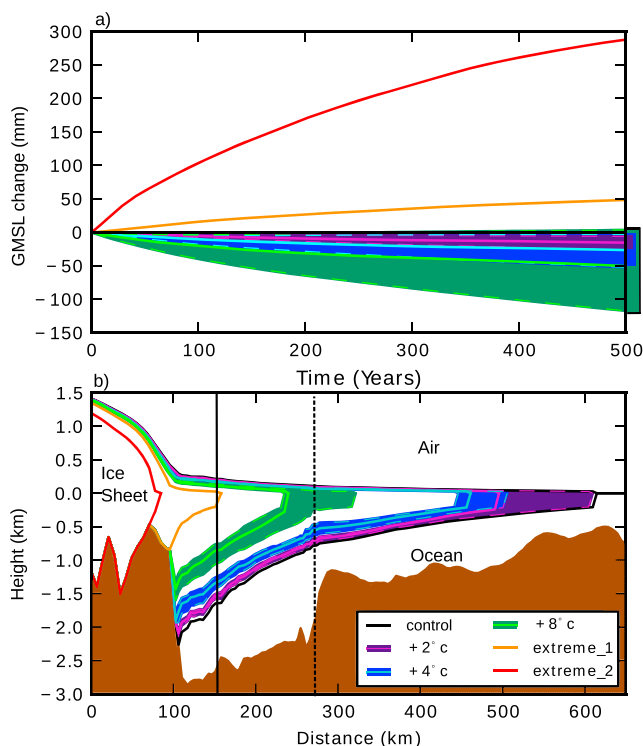


Figure 2. (a) Relative GMSL change with respect to the control solution out to 500 years. Lines reflect the middle scenario for each temperature case, as indicated by colors referring to legend in Figure 2b. Dashed lines and shaded regions show the extent of the lower and upper scenarios, respectively. (b) Cross section along the Lambert Glacier and Amery Ice Shelf following the transect shown in green, Figure 1b). The approximate locations of the MISW and the end of compressional flow are shown as vertical solid and dashed lines, respectively.

matches a simulation from the previous sensitivity study in the region [Gong *et al.*, 2014] in addition to testing the risk of retreat into the marine basins.

All changes are applied in boundary conditions as a step change at the beginning of the simulation. This was required as the variations in *bmelt* were restricted to step changes, as time varying *bmelt* fields from an uncoupled ocean model would not track the grounding line position. The consequence of the step change in our scenarios is that they will likely overestimate GMSL change throughout the first 100 years of the simulation, as in reality the changes would be gradually changing over this period, rather than occurring as a step change. However, we contend that the simulations provide a plausible bound for GMSL change over the next 500 years for Lambert-Amery glacial system, given our choice in model parameterizations and future climate scenarios. We also suggest that our simulations, as they overestimate possible GMSL, should test the risk of rapid collapse into the marine basin.

3. Results

The simulated climate scenarios all yielded a decrease in sea level over the 500 year period (Figure 2a), with a change of -15.6 ($+2^{\circ}\text{C}$ middle scenario), -26.7 ($+4^{\circ}\text{C}$ middle scenario) and -50.6 ($+8^{\circ}\text{C}$ middle scenario) mm GMSL equivalent. The drift in the control simulation was -3.75 mm which has been corrected for in all simulations. As the temperature scenarios increase, the gain in mass was diminishing as a function of temperature, with a rate of 7.8 mm GMSL equivalent per degree for $+2^{\circ}\text{C}$, but a rate of only 6.3 mm GMSL equivalent per degree for $+8^{\circ}\text{C}$. The upper scenario simulations estimated near zero change, with -6.2 ($+2^{\circ}\text{C}$ upper scenario), -3.2 ($+4^{\circ}\text{C}$ upper scenario), and $+3.6$ ($+8^{\circ}\text{C}$ upper scenario) mm GMSL-equivalent change over the 500 years. Note the $+8^{\circ}\text{C}$ upper scenario had risen from -2.4 mm SLR equivalent at 200 years, indicating it was losing mass at the end of the simulation. The lower scenario-simulated estimated mass gain of -26.7 ($+2^{\circ}\text{C}$ lower scenario), -52.3 ($+4^{\circ}\text{C}$ lower scenario) and -117.5 ($+8^{\circ}\text{C}$ lower scenario) mm SLR equivalent, indicating that increased snowfall drives the changes in GMSL. The extreme scenarios led to sea level change of $+48.2$ (extreme_1) and $+287.9$ (extreme_2) mm GMSL equivalent. The majority of the change occurred within the

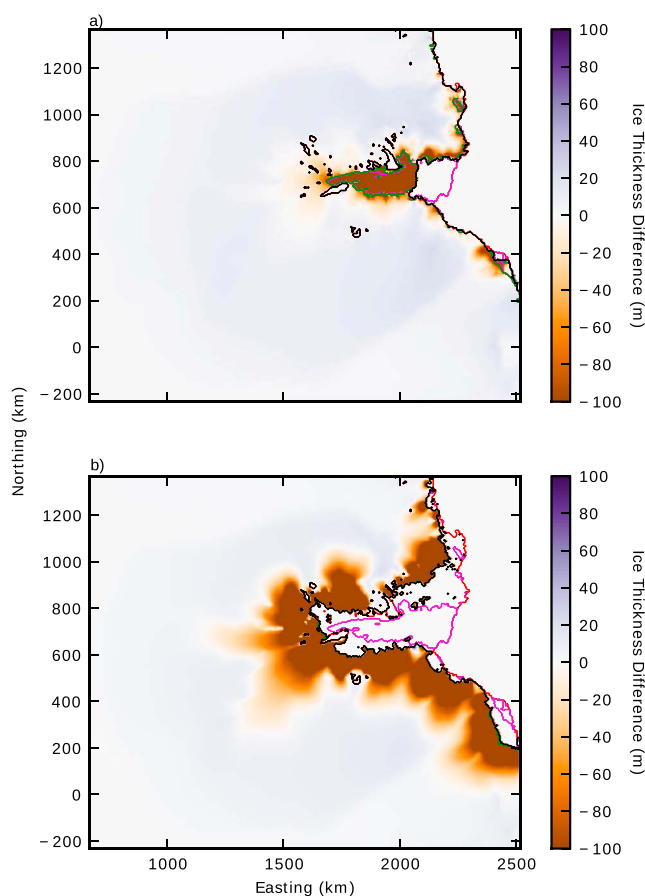


Figure 3. Ice thickness difference compared to the control solution for (a) middle $+4^{\circ}\text{C}$ scenario and (b) extreme_2 scenario. The control ice shelf mask is indicated in magenta and the ice free mask in red. The scenario ice shelf mask is indicated in green and the ice free mask in black.

first 200 years, with 55% and 59% of the overall GMSL change occurring within this period, with the remainder occurring over the last 300 years. This suggests the system was moving slowly toward a new equilibrium state.

In all scenarios, the regions of at high elevation with small ice velocities gained mass, while the mass loss primarily occurred in the faster-flowing glaciers near the grounding line (Figure 3), which creates a steeper surface gradient. In all simulations, the calving front has retreated into the embayment, varying from just over 100 km of retreat for the $+2^{\circ}\text{C}$ middle scenario to over 350 km in the $+8^{\circ}\text{C}$ middle scenario. The extreme_2 scenario has lost substantially more ice, with the retreat of the grounding line along the edges of the Amery Ice Shelf (Figure 3), which is also seen in the $+8^{\circ}\text{C}$ and extreme_1 scenarios. However, the substantial retreat into the marine grounded portion of the Fisher Glacier basin is unique to the Extreme_2 scenario and implies that out of the three major tributaries, the Fisher is the most unstable.

The thinning, retreat, and removal of the ice shelf causes acceleration in the glacial flow of the primary tributary glaciers, with the average increase in grounded ice surface velocities observed 80 km upstream of the initial grounding line. The initial velocity increases in the simulations after 50 years was 186%, 54%, and 75% for the extreme_2 scenario within the Fisher, Lambert and Mellor Glaciers, respectively. The velocity increases reached a maximum of 73% after 300 years for the Lambert Glacier, and a maximum of 101% for the Mellor Glacier after 250 years. The final velocities after 500 years of the simulation are 41% and 44%, for the Lambert and Mellor Glaciers, respectively. This indicates that after an acceleration throughout the simulation, the surface velocities begin to decrease before the end of the simulation. The increases are significantly less in simulations where a small ice shelf remains, with the surface velocity in the $+8^{\circ}\text{C}$ middle scenario only 55%, 13%, and 13% for the Fisher, Lambert, and Mellor glaciers after 50 years, increasing in velocity up to 72%, 22%, and 15% over the full simulation.

4. Discussion

The projected mitigation of SLR in each of the scenarios investigated here (with the exception of extreme_2) is driven by the increase in mass at high elevations exceeding the dynamic losses due to increased flow across the grounding line. Two significant factors in the pattern of change seen in all scenarios is that the calving front did not retreat past the MISW (excluding the extreme_2 scenario), and the grounding line was unable to retreat over the shallow sill (at 100 km on Figure 2b) into regions grounded below sea level. The only scenario to retreat into the marine basins was extreme_2, which retreated into the Fisher basin, the smallest of the three major tributary glaciers (Figure 3b).

The distance the calving front retreated increased as the scenarios increased in global temperature. In the +8°C middle and upper scenario simulation, the calving front retreated ~350 km into the embayment. While a 350 km retreat is over half the initial length of the ice shelf, the calving front is still north of the MISW and Clemence Massif (Figure 1b). The horizontal compression occurring in the region between the grounding line and the MISW can be seen in the profile of the ice shelf (ice shelf left of vertical dashed line in Figure 2b).

The ice shelf remains thicker between the compression point and the grounding line relative to an idealized ice shelf due to a reduction in velocity from the buttressing at the MISW and the compressional flow occurring up until the location indicated on Figure 2b. This suggests that the region south of both Clemence Massif and the MISW provides a significant portion of the upstream buttressing from the Amery Ice Shelf. We find that in the extreme_2 scenario, where the entire ice shelf was removed, significantly faster upstream velocities are present when compared to any scenario which has a remaining ice shelf. These findings are supported by *Gong et al.* [2014] who found that only once the calving front retreated past Clemence Massif could significant upstream increases in velocity occur.

The extreme scenarios led to an increase in GMSL, with the ice shelf retreating past the MISW and Clemence Massif in both cases, and the complete collapse of the ice shelf in the extreme_2 scenario. The average melt rate in the +8°C upper scenario was 5.4 m yr⁻¹, the extreme_1 and 2 scenarios were 10.4 m yr⁻¹ and 100.2 m yr⁻¹, respectively. While the average melt rate within the temperature scenarios are lower than observed in some of the coastal ice shelves in the Amundsen Sea sector [*Rignot et al.*, 2014], it is higher than the modelled increases in oceanic basal melt on the Filchner-Ronne Ice shelf [*Hellmer et al.*, 2012].

However, given the partial and complete collapse in the two extreme scenarios, increasing the melt rate further will not yield different results. The difference in GMSL change between the middle +4°C and the extreme_2 (which used the +4°C surface temperature and surface mass balance) highlights the importance of the last ~100 km of ice shelf to buttressing the upstream ice flow.

These results show greater variability than a previous regional study [*Gong et al.*, 2014], which found that the Lambert-Amery glacial system had a GMSL change range of -15 and 11 mm GMSL equivalent over a simulation spanning 1980–2200. In our simulations we found a GMSL change range of -43 and +32 mm GMSL equivalent over the initial 200 years. Some of these differences will be due to the forcing applied, with *Gong et al.* [2014] using regional atmospheric and oceanic models to force their model over the 200 years; however, they included an extreme scenario with an ice shelf-wide oceanic basal melt rate of 100 m yr⁻¹ which is comparable to our extreme_2 scenario that is included in the comparison.

It is difficult to directly compare the loss from our regional model to that of whole Antarctic models as they do not provide a basin by basin breakdown of change. In both *Golledge et al.* [2015] and *DeConto and Pollard* [2016], the grounding line appears to be further retreated than in both *Gong et al.* [2014] and our simulations. Both *Gong et al.* [2014] and our study agreed, in that the grounding line of the Amery Ice Shelf was unable to retreat into the retrograde beds, which contrasted with the whole Antarctic models.

The differences in grounding line stability between the low-resolution whole Antarctic models, which retreated significantly further inland, and the high-resolution regional models, which stabilized on a shallow sill, could be a cause for concern. The poorly constrained bed topography (noting our requirement to modify Bedmap2 to remove erroneous data near the grounding line), will undoubtedly influence the evolution of the ice sheet in the simulations. The regional study of *Gong et al.* [2014] uses ALBMAP [*Le Brocq et al.*, 2010], which utilized similar bed topography beneath the Amery Ice Shelf than in our simulations but will suffer

from the lack of significant marine basins identified in Bedmap2. Both *Golledge et al.* [2015] and *DeConto and Pollard* [2016] use Bedmap2, which include the unrealistically shallow topography immediately adjacent to the grounding line.

The difference in the extent of grounding line retreat could also be directly linked to smoothing of the bed topography in the coarser resolution models. The bed topography rises relatively steeply into the shallow sill (at 100 km in Figure 2b), which in coarse resolution models will be smoothed out over a coarser (20 km) footprint, which will lead to a deeper sill. This would allow for a higher mass flux to occur across a deeper grounding line, increasing the rate at which the system can lose mass and subsequently sustain grounding line retreat further inland. This will have a significant impact on their ability to realistically model the Lambert-Amery glacial system, and likely other regions of the East Antarctic ice sheet. If other regional systems across East Antarctica are also being poorly constrained in coarse whole Antarctic models, then these regions may potentially also help mitigate the probable positive contribution to GMSL change from Antarctica.

Our results also contrast with *Winkelmann et al.* [2012] who found that increased surface velocities in a warmer climate mitigated the possible mass gain from increased precipitation with an increase in the through-flow of ice. This difference could have been caused by different parameterization of the ice rheology, specifically the shallow ice enhancement factor (*sia_e*). *Winkelmann et al.* [2012] used a *sia_e* of 4.5, which compares to the lower values of 1.8 [*Pittard et al.*, 2016a] used in our simulations. The use of a lower value for the *sia_e* is supported by *Golledge et al.* [2015] and *Aschwanden et al.* [2016], which used values in the range 1 to 1.5 for this parameter. We found a substantially better fit to observations using lower *sia_e* values, with higher values leading to ice surface velocities at high elevations (2000+) both exceeding the mean by at least 25% and leading to a reduction in ice thicknesses at high elevations [*Pittard*, 2016]. This difference will directly influence the flow of ice at high elevations, where our simulations experienced the majority of their mass gain. The use of a high *sia_e* led to increased velocities at high elevations, which will allow for faster transport of mass to the grounding line. This may suggest the through-flow is sensitive to the chosen enhancement factor of the shallow ice approximation.

The PISM ice sheet model does not include the hydrofracture and ice cliff failure mechanisms [*Pollard et al.*, 2015], both of which have been suggested as mechanisms that may lead to additional retreat [*DeConto and Pollard*, 2016]. The hydrofracture mechanism depends on the presence of surface melt as well as the divergence in the flow of the ice shelf to generate and sustain crevasses [*Pollard et al.*, 2015], while the ice cliff failure mechanism depends on the complete removal of the ice shelf. The Amery Ice Shelf should be resistant to hydrofracture and ice cliff failure, as the region between the grounding line and the MISW region experiences convergent flow, which would act to close, rather than continue to open any crevasses. This is supported by the attempt to correlate surface features for velocity measurements [*Pittard et al.*, 2013], which is unable to track many surface features throughout this region. This suggests that the surface features are significantly different from those upstream. We suspect that the compressional flow is responsible for these changes, closing the upstream crevasses and reducing coherence between image pairs as shown by *Pittard et al.* [2013].

The risk of the ice cliff failure mechanism occurring near the current grounding line is uncertain. The maximum height of the bedrock topography which the grounding line would retreat over is -500 m below sea level. The threshold for triggering ice cliff failure is still relatively uncertain, with current estimates in bedrock topography ranging between -450 and -800 m [*Ma et al.*, 2017; *Pollard et al.*, 2015]. Given the uncertainty in both the height required to trigger ice cliff failure and the bedrock topography itself, it is difficult to assess the risk from this mechanism.

Additionally, current implementations of the ice cliff failure mechanism do not account for the possibility of the formation of an ice mélange that may form in the region that was occupied by the former ice shelf. An ice mélange has been attributed to the reduced mass loss from the Jakobshavn Glacier during the winter months when the ice mélange is at its strongest [*Amundson et al.*, 2010]. The buttressing from the ice mélange helps to stabilize the ice cliff, reducing the rate of calving. The unique geography of the embayment associated with the Amery Ice Shelf may aid in the development of an ice mélange and thus mitigate possible losses from the ice cliff mechanism. There is evidence to suggest that tidewater glaciers may have existed within this region in the past [*McKelvey et al.*, 2001]; however, they would have been located north of the Clemence Massif, indicating that the grounding line was in an advanced position. The current grounding line could be a relatively recent consequence of substantial erosion through the glacial-interglacial cycles [*Taylor et al.*, 2004], making paleo-assessments of the response to warming difficult.

For substantial mass loss to occur from the Lambert-Amery glacial system, the grounding line must retreat over the shallow sill which is upstream of where it is presently grounded. For this retreat to occur, it would require the velocity over the grounding line to increase to ensure that the flux is increasing, even though the ice thickness is decreasing as the grounding line moves onto shallower bed topography. In our simulations, this was unable to occur, even in the extreme scenarios where the ice shelf was completely removed. The depth and shape of this sill is therefore fundamentally important to the stability of the region. The modifications to Bedmap2 in this study include a 5 km region north of the grounding line where interpolation is used to merge the two input bed topography data sets. Further observations of the bed topography and, in particular, the height and shape of the sill where the grounding line is currently located are important to improve the estimations of sea level change from the Lambert-Amery glacial system.

5. Conclusion

Using a number of future climate scenarios, our simulations of the Lambert-Amery glacial system show that the grounding line is unlikely to retreat beyond the topographic sill where the present-day grounding line occurs over the next 500 years. Our results suggest that this will limit the possible increased dynamic mass loss from the Lambert-Amery glacial system in a warming climate, allowing for the expected increases in precipitation to cause an overall net mass gain across the region. We find that only in the most extreme scenario could the grounding line be forced to retreat into the marine grounded ice, with the rapid retreat of the grounding line into the Fisher Glacier, the smallest of the three marine basins. Overall, the extreme_2 scenario contributed +287.9 mm GMSL-equivalent rise over 500 years, a sharp increase from the extreme_1 scenario of +48.2 mm GMSL equivalent. It is important to improve our knowledge of the bed topography near and behind the grounding line, as the retreat was stabilized by shallow sills which restrict the maximum mass flux across the grounding line. If these sills are substantially deeper than we currently believe, the grounding line may be more susceptible to rapid retreat.

Under all temperature increase scenarios, a modest-sized ice shelf remained, contributing significant buttressing to the three main tributary glaciers. The stability of the grounding line combined with the buttressing of the ice shelf limited the dynamic response of the Lambert-Amery glacial system, leading to a net mass gain given elevated surface mass balance. We conclude that the Lambert-Amery glacial system region will likely remain stable or gain ice mass and mitigate a portion of potential future sea level rise. A global increase in temperature of +2°C led to an increase in mass, resulting in a sea level fall of −15.6 mm GMSL equivalent, with a +4°C and +8°C increase leading to −26.7, −50.6 mm GMSL equivalent, respectively. When considering the possible bounds of each simulation, we suggest that the overall range of GMSL change from the Lambert-Amery glacial system will be within +3.6 to −117.5 mm GMSL equivalent over the next 500 years.

Acknowledgments

This work was supported by and Australian Government's Cooperative Research Centres programme through the Antarctic Climate & Ecosystems Cooperative Research Centre (ACE CRC). This research was supported under Australian Research Council's Special Research Initiative for Antarctic Gateway Partnership (Project ID SR140300001). This research was undertaken with the assistance of resources under projects m68 and gh8 from the National Computational Infrastructure (NCI), which is supported by the Australian Government. Development of PISM is supported by NASA grants NNX13AM16G and NNX13AK27G. All data sets, scripts, and outputs used to generate these results will be available through the Australian Antarctica Data Center (<https://data.aad.gov.au/>)

References

- Amundson, J. M., M. Fahnestock, M. Truffer, J. Brown, M. P. Lüthi, and R. J. Motyka (2010), Ice mélange dynamics and implications for terminus stability, Jakobshavn Isbræ, Greenland, *J. Geophys. Res.*, *115*, F01005, doi:10.1029/2009JF001405.
- Aschwanden, A., E. Bueler, C. Khroulev, and H. Blatter (2012), An enthalpy formulation for glaciers and ice sheets, *J. Glaciol.*, *58*(209), 441–457, doi:10.3189/2012JoG11J088.
- Aschwanden, A., M. A. Fahnestock, and M. Truffer (2016), Complex Greenland outlet glacier flow captured, *Nat. Commun.*, *7*, 10524, doi:10.1038/ncomms10524.
- Bueler, E., and J. Brown (2009), Shallow shelf approximation as a "sliding law" in a thermomechanically coupled ice sheet model, *J. Geophys. Res.*, *114*, F03008, doi:10.1029/2008JF001179.
- DeConto, R. M., and D. Pollard (2016), Contribution of Antarctica to past and future sea-level rise, *Nature*, *531*(7596), 591–597, doi:10.1038/nature17145.
- Favier, L., O. Gagliardini, G. Durand, and T. Zwinger (2012), A three-dimensional full Stokes model of the grounding line dynamics: Effect of a pinning point beneath the ice shelf, *Cryosphere*, *6*, 101–112, doi:10.5194/tc-6-101-2012.
- Feldmann, J., T. Albrecht, C. Khroulev, F. Pattyn, and A. Levermann (2014), Resolution-dependent performance of grounding line motion in a shallow model compared with a full-Stokes model according to the MISMIP3d intercomparison, *J. Glaciol.*, *60*, 353–360, doi:10.3189/2014JoG13J093.
- Fox Maule, C., M. E. Purucker, N. Olsen, and K. Mosegaard (2005), Heat flux anomalies in Antarctica revealed by satellite magnetic data, *Science*, *309*(5733), 464–467, doi:10.1126/science.1106888.
- Fretwell, P., et al. (2013), Bedmap2: Improved ice bed, surface and thickness datasets for Antarctica, *Cryosphere*, *7*, 375–393, doi:10.5194/tc-7-375-2013.
- Galton-Fenzi, B. (2009), Modelling ice-shelf/ocean interaction, PhD thesis, Univ. of Tasmania, Hobart, Australia.
- Galton-Fenzi, B., C. Maraldi, R. Coleman, and J. Hunter (2008), The cavity under the Amery ice shelf, East Antarctica, *J. Glaciol.*, *54*(188), 881–887, doi:10.3189/002214308787779898.
- Galton-Fenzi, B. K., J. R. Hunter, R. Coleman, S. J. Marsland, and R. C. Warner (2012), Modeling the basal melting and marine ice accretion of the Amery ice shelf, *J. Geophys. Res.*, *117*, C09031, doi:10.1029/2012JC008214.

- Gladstone, R. M., A. J. Payne, and S. L. Cornford (2010), Parameterising the grounding line in flow-line ice sheet models, *Cryosphere*, *4*, 605–619, doi:10.5194/tc-4-605-2010.
- Golledge, N. R., D. E. Kowalewski, T. R. Naish, R. H. Levy, C. J. Fogwill, and E. G. W. Gasson (2015), The multi-millennial Antarctic commitment to future sea-level rise, *Nature*, *526*, 421–425, doi:10.1038/nature15706.
- Gong, Y., S. L. Cornford, and A. J. Payne (2014), Modelling the response of the Lambert Glacier-Amery Ice Shelf system, East Antarctica, to uncertain climate forcing over the 21st and 22nd centuries, *Cryosphere*, *8*(3), 1057–1068, doi:10.5194/tc-8-1057-2014.
- Hellmer, H. H., F. Kauker, R. Timmermann, J. Determann, and J. Rae (2012), Twenty-first-century warming of a large Antarctic ice-shelf cavity by a redirected coastal current, *Nature*, *485*, 225–228, doi:10.1038/nature11064.
- Huybrechts, P. (2002), Sea-level changes at the LGM from ice-dynamic reconstructions of the Greenland and Antarctic ice sheets during the glacial cycles, *Quat. Sci. Rev.*, *21*, 203–231, doi:10.1016/S0277-3791(01)00082-8.
- Le Brocq, A. M., A. J. Payne, and A. Vieli (2010), An improved Antarctic dataset for high resolution numerical ice sheet models (ALBMAP v1), *Earth Syst. Sci. Data*, *2*, 247–260, doi:10.5194/eesd-2-247-2010.
- Ma, Y., C. S. Tripathy, and J. N. Bassis (2017), Bounds on the calving cliff height of marine terminating glaciers, *Geophys. Res. Lett.*, *44*, 1369–1375, doi:10.1002/2016GL071560.
- Martin, M. A., R. Winkelmann, M. Haseloff, T. Albrecht, E. Bueler, C. Khroulev, and A. Levermann (2011), The Potsdam Parallel Ice Sheet Model (PISM-PIK)—Part 2: Dynamic equilibrium simulation of the Antarctic ice sheet, *Cryosphere*, *5*, 727–740, doi:10.5194/tc-5-727-2011.
- McKelvey, B. C., M. J. Hambrey, D. M. Harwood, M. C. G. Mabin, P.-N. Webb, and J. M. Whitehead (2001), The Pagodroma Group—A Cenozoic record of the East Antarctic ice sheet in the northern Prince Charles Mountains, *Antarctic Sci.*, *13*(4), 455–468, doi:10.1017/S095410200100061X.
- O’Gorman, P. A., and C. J. Muller (2010), How closely do changes in surface and column water vapor follow Clausius-Clapeyron scaling in climate change simulations?, *Environ. Res. Lett.*, *5*(2), 25207, doi:10.1088/1748-9326/5/2/025207.
- Pachauri, R. K., et al. (2014), *Climate Change 2014: Synthesis Report. Contribution of Working Groups I, II and III to the Fifth Assessment Report of the Intergovernmental Panel on Climate Change*, 151 pp., IPCC, Geneva, Switzerland.
- Pattyn, F., et al. (2012), Results of the Marine Ice Sheet Model Intercomparison Project, MISMP, *Cryosphere*, *6*, 573–588, doi:10.5194/tc-6-573-2012.
- Pittard, M. L. (2016), The dynamics of the Lambert-Amery glacial system and its response to climatic variations, PhD thesis, Univ. of Tasmania, Hobart, Australia.
- Pittard, M. L., J. L. Roberts, R. C. Warner, B. K. Galton-Fenzi, C. S. Watson, and R. Coleman (2013), Flow of the Amery ice shelf and its tributary glaciers, in *18th Australasian Fluid Mechanics Conference*, vol. 1, pp. 605–608, Curran Associates, Inc., Launceston, Tasmania.
- Pittard, M. L., B. K. Galton-Fenzi, J. L. Roberts, and C. S. Watson (2016a), Organization of ice flow by localized regions of elevated geothermal heat flux, *Geophys. Res. Lett.*, *43*, 3342–3350, doi:10.1002/2016GL068436.
- Pittard, M. L., J. L. Roberts, B. K. Galton-Fenzi, and C. S. Watson (2016b), Sensitivity of the Lambert-Amery glacial system to geothermal heat flux, *Ann. Glaciol.*, *57*, 56–68, doi:10.1017/aog.2016.26.
- Pollard, D., R. M. DeConto, and R. B. Alley (2015), Potential Antarctic ice sheet retreat driven by hydrofracturing and ice cliff failure, *Earth Planet. Sci. Lett.*, *412*, 112–121, doi:10.1016/j.epsl.2014.12.035.
- Rignot, E., J. Mouginot, M. Morlighem, H. Seroussi, and B. Scheuchl (2014), Widespread, rapid grounding line retreat of Pine Island, Thwaites, Smith, and Kohler glaciers, West Antarctica, from 1992 to 2011, *Geophys. Res. Lett.*, *41*, 3502–3509, doi:10.1002/2014GL060140.
- Taylor, J., M. J. Siebert, A. J. Payne, M. J. Hambrey, P. E. O’Brien, A. K. Cooper, and G. Leitchenkov (2004), Topographic controls on post-Oligocene changes in ice-sheet dynamics, Prydz Bay region, East Antarctica, *Geology*, *32*, 197, doi:10.1130/G20275.1.
- Timmermann, R., et al. (2010), A consistent data set of Antarctic ice sheet topography, cavity geometry, and global bathymetry, *Earth Syst. Sci. Data*, *2*(2), 261–273, doi:10.5194/eesd-2-261-2010.
- van Wessem, J. M., et al. (2014), Improved representation of East Antarctic surface mass balance in a regional atmospheric climate model, *J. Glaciol.*, *60*, 761–770, doi:10.3189/2014JoG14J051.
- Winkelmann, R., M. A. Martin, M. Haseloff, T. Albrecht, E. Bueler, C. Khroulev, and A. Levermann (2011), The Potsdam Parallel Ice Sheet Model (PISM-PIK)—Part 1: Model description, *Cryosphere*, *5*(3), 715–726, doi:10.5194/tc-5-715-2011.
- Winkelmann, R., A. Levermann, M. A. Martin, and K. Frieler (2012), Increased future ice discharge from Antarctica owing to higher snowfall, *Nature*, *492*, 239–242, doi:10.1038/nature11616.